Biological Journal of the Linnean Society, 2020, **129**, 603–617. With 7 figures.

Phylogeographical spatial diffusion analysis reveals the journey of Geoffroy's cat through the Quaternary glaciations of South America

MARÍA JIMENA GÓMEZ FERNÁNDEZ, ALBERTO FAMELI, JULIO ROJO GÓMEZ, JAVIER A. PEREIRA and PATRICIA MIROL*

Grupo de Genética y Ecología en Conservación y Biodiversidad, División Mastozoología, Museo Argentino de Ciencias Naturales 'Bernardino Rivadavia', CONICET. Ángel Gallardo 470, 1425, Buenos Aires, Argentina

Received 10 October 2019; revised 18 December 2019; accepted for publication 19 December 2019

Leopardus geoffroyi is a small feline with a widespread distribution in a broad array of habitats. Here we investigate its evolutionary history to characterize the phylogeographical patterns that led to its present distribution using mitochondrial DNA from 72 individuals collected throughout its entire range. All haplotypes conformed to a monophyletic group, including two clades with a central/marginal disposition that is incongruent to the proposed subspecies. Spatial diffusion analysis showed the origin of the species within the oldest and more diverse central clade. A Bayesian Skyline Plot combined with a dispersal through time plot revealed two population increases at 190 000–170 000 and 45 000–35 000 years ago, the latter period accompanied by an increase in the dispersal rate. Species distribution models showed similar patterns between the present and Last Interglacial Period, and a reduction of high-probability areas during the Last Glacial Maximum (LGM). Molecular evidence confirms *L. geoffroyi* as a monotypic species whose origin is located in Central Argentina. The last glaciation had little effect on the pattern of distribution of the species: the population and range expansion that started before the LGM, although probably being halted, continued after the glaciation and resulted in the presence of this felid in the far south of Patagonia.

ADDITIONAL KEYWORDS: *Leopardus geoffroyi*, mitochondrial DNA, Quaternary glaciations, South America, spatial diffusion analysis, species distribution modelling

INTRODUCTION

South America harbours 11 species of wild felids, representing 27% of the global diversity of this group (Kitchener *et al.*, 2017; but see Nascimento & Feijó, 2017 and Ruiz-García *et al.*, 2017 for two other possible species recently described). Eight of these species are included in the 'Ocelot' lineage and are currently placed in a single genus, *Leopardus*, based on the recent radiation, natural hybridization and the close similarity in skull morphology between them (Johnson *et al.*, 2006; Kitchener *et al.*, 2017). The most common felid species of this genus in the southern cone of South America is Geoffroy's cat *Leopardus geoffroyi* (D'Orbigny & Gervais, 1844), a small feline (~4–5 kg) with a widespread and continuous distribution from Bolivia and Brazil to southern Patagonia in Argentina and Chile (Pereira *et al.*, 2015). This species lives in a broad array of natural habitats, including scrublands, dry forests, savannas, grasslands, marshlands and steppes of the subtropical and temperate Neotropics, from 0 to 3800 m a.s.l. (Cuyckens *et al.*, 2016). Geoffroy's cat exhibits behavioural plasticity, exploiting human-dominated habitats, and it is currently categorized as of Least Concern by the IUCN (Pereira *et al.*, 2015).

Based on the morphological studies of Pocock (1940), Cabrera (1958) and Ximenez (1973), four subspecies of Geoffroy's cat were recognized by Ximenez (1975): *L. g. geoffroyi* (D'Orbigny & Gervais, 1844) in Patagonia and central Argentina; *L. g. salinarum* (Thomas, 1903) in north-western Argentina; *L. g. paraguae* (Pocock, 1940) in southern Brazil, Uruguay, and eastern Argentina and Paraguay; and *L. g. euxanthus* (Pocock, 1940) in Bolivia and northern Argentina. Johnson *et al.* (1999)

*Corresponding author. E-mail: pmirol@macn.gov.ar

subsequently revisited the taxonomy of Geoffroy's cat by assessing patterns of DNA sequence variation using three mitochondrial genes (*16S* rRNA, *ATP8* and *NADH-5*) and 20 microsatellite loci of 38 captive specimens throughout its distribution. These authors found a lack of geographical structure in the species and estimated that extant lineages of *L. geoffroyi* diverged 2.0 Mya. Furthermore, Nascimento (2014) reassessed Geoffroy's cat taxonomic units by using external and craniodental morphology in a sample of 200 specimens housed in museums, detecting a high degree of morphological variation but no evidence of any subspecific division. Kitchener *et al.* (2017) proposed that three lines of correlated evidence are required to support a given taxonomy: morphological, genetic and biogeographical. Given the knowledge available on *L. geoffroyi* at that time, they suggested that 'until further genetic data are available, it is probably best to treat *L. geoffroyi* as a monotypic species' (p. 57, Kirtchener *et al.*, 2017).

A well-supported taxonomy is critical to determining the conservation status of any group of organisms. The phylogenetic approach is now commonly used to establish species/subspecies limits based on reciprocal monophyly. However, there are numerous examples of incongruence between these inferences and those derived from other sources such as morphology (Knowles & Carstens, 2007). Indeed, gene trees cannot always be equated to species trees. Instead, they should be combined with historical information and the evolutionary context and dynamics of the lineage in order to establish its taxonomy.

One of the major breakpoints in the evolutionary history of many species of plants and animals were the glaciations of the Quaternary. The effects of these glaciations on the evolution of biodiversity have been extensively studied in the Northern Hemisphere (Hewitt, 2000, 2004) but remain neglected for the Southern Hemisphere. One of the many reasons for this lack of information is that only 32% of the Earth's land area is located in the Southern Hemisphere. The extension of glaciers was not as large as in the north, occupying only portions of Patagonia close to the Andes and leaving most of Argentinean Patagonia and Chile unglaciated during the Late Pleistocene (Clapperton, 1993; Rabassa *et al.*, 2000). Moreover, the area covered by glaciers during the Last Glacial Maximum (LGM) was compensated for by the exposure of a large continental shelf in the Southern Atlantic (Rabassa *et al.*, 2000). However, glaciation cycles in South America, with the subsequent climate change, produced dramatic effects even as far north as the Amazon (Turchetto-Zolet *et al.*, 2013). It has been argued that Quaternary glaciations have been ultimately responsible for the diversification of the immense biodiversity of South America, driving speciation and within-species differentiation (Cosacov Martínez *et al.*, 2010; Lessa *et al.*, 2010; Sersic *et al.*, 2011; Camargo *et al.*, 2013; Turchetto-Zolet *et al.*, 2013). It is thus of interest to test how glacial cycles could have affected the evolutionary history of a species with a broad distribution and, in particular, with ecological plasticity to occupy such a variety of habitats as with Geoffroy's cat. The results of these analyses would also provide details of the evolutionary processes through the history of the species that would have determined its current distribution and, ultimately, taxonomy.

Climate change, such as the Quaternary glaciations, produced a number of demographic variations in populations and species: changes in population size and geographical range, local extinctions and colonizations. Molecular markers have proved to be excellent proxies to reconstruct such changes. Nowadays, the use of molecular markers in Bayesian approaches for spatio-temporal phylogeographical reconstruction allows inferences to be made regarding the geographical location of ancestors using models of geographical diffusion over space and time (Drummond *et al.*, 2012). Because the diffusion process is coupled with phylogeny, it is possible to estimate and compare demographic and geographical expansion models (Lemey *et al.*, 2009, 2010). Adding species distribution models (SDMs) (Phillips *et al.*, 2006; Elith & Leathwick, 2009; Elith *et al.*, 2010) to the phylogeographical approaches that integrate geospatial methods can help to understand the evolutionary mechanisms driving population history.

In this study we investigate the evolutionary history of *L. geoffroyi* using mitochondrial DNA (mtDNA) to characterize the phylogeographical patterns that led to its current distribution. We use a large dataset covering the entire geographical range of the species to perform explicit phylogeographical analyses using spatial diffusion models and project these to understand the incidence of past major climate changes. We expect to clarify Geoffroy's cat taxonomy not only through a molecular phylogeny but also by including its demographic history.

MATERIAL AND METHODS

Sampling and genetic data

We assessed sequence variation in mtDNA for 72 individuals collected throughout the range of *L. geoffroyi* in Bolivia, Brazil, Uruguay and Argentina (Fig. 1). An area of extensive hybridization between *L. geoffroyi* and *L. guttulus* has been identified at their geographical contact zone in southern Brazil (Trigo *et al.*, 2008). To avoid including samples of potential hybrids that may influence our analysis, samples of 'pure' Geoffroy's cats from Brazil were provided by T. Trigo.

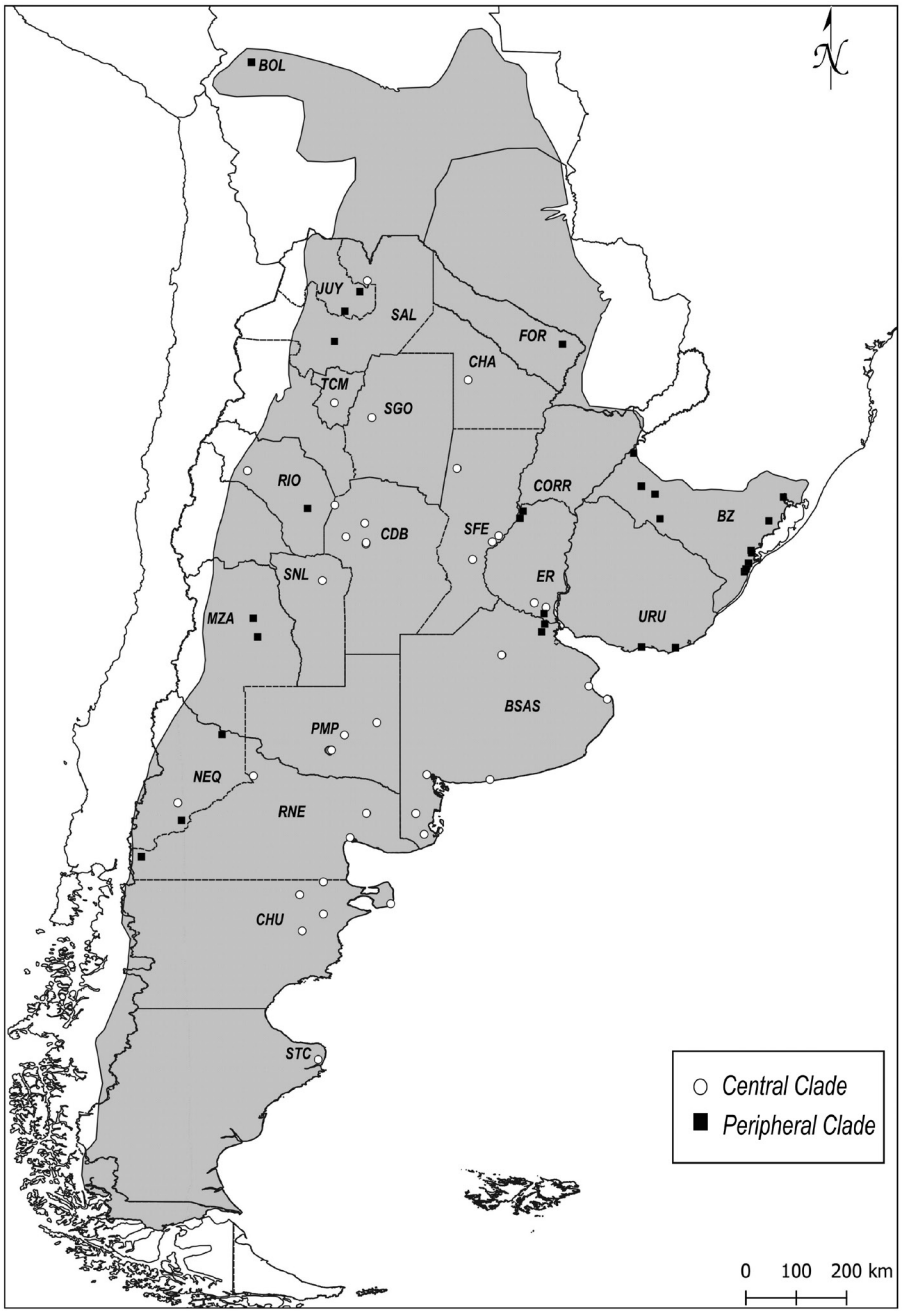

Figure 1. Samples collected for the study. In grey, the distribution range of *Leopardus geoffroyi* according to Cuyckens *et al* (2016). Black squares, Peripheral Clade; white circles, Central Clade. The abbreviations identify the geographical areas, and are included in Supporting Information Table S1.

Muscle samples were collected from road-killed animals and preserved in 96% ethanol, while blood samples were obtained from wild animals captured for ecological studies and kept in Tris-EDTA. Museum samples consisted of ~0.5 cm^2 of footpads or skin. We extracted DNA from blood using DNAzol (ThermoFisher Scientific) following the manufacturer instructions, and from other tissues by following a modified SDS–proteinase K–ClNa protocol (Miller *et al.*, 1988), with a previous wash and hydration step with NaCl 100 mM, Tris-HCl 10 mM, EDTA 1mM (TNE) solution for museum samples.

We amplified 1306 bp comprising a fragment of the *NADH* gene (*NAD*, primers ND5-DF1 and ND5-DR1, Trigo *et al.*, 2008) and two fragments of the *Control Region* (*CR*, primers Thr-L 5′-GAA

TTCCCCGGTCTTGTAAACC-3′ and DH-L 5′-CCTGAACTACGAACCAGATG-3′ modified from Kocher *et al.*, 1989). We sequenced the *CR* in two separate fragments to avoid amplification of a repetitive region that produces heteroplasmy. PCR amplifications for all fragments were performed in a final volume of 20 µL, containing DNA template (1–2 µL), 0.4 µM each primer, 0.2 mM dNTP, 1× KAPA2G Buffer A, 1.5 mM $MgCl_2$, 0.2 mg/mL BSA and 0.03 units of KAPA2G Fast DNA Polymerase (KAPA Biosystems). The cycling for *CR* consisted of 94 °C for 5 min, followed by 10 cycles of denaturing at 94 °C for 40 s and annealing at 65 °C for 20 s, with 1 °C decrements at every cycle. This was followed by 10 cycles of denaturing at 94 °C for 40 s and annealing at 56 °C for 20 s, and finally 20 cycles of denaturing at 94 °C for 20 s and annealing at 54 °C for 10 s For *NAD* the cycling protocol consisted of 94 °C for 5 min, followed by 12 cycles of denaturing at 94 °C for 40 s, annealing at 58 °C for 20 s with 1 °C decrements from 58 to 46 °C at every cycle, and 30 cycles of denaturing at 94 °C for 40 s and annealing at 48 °C for 30 s Negative controls were included in all PCR runs to check for contamination.

We visualized PCR products on 1.2% agarose gels and purified the amplicons with the enzymes Exonuclease I and Shrimp Alkaline Phosphatase (ThermoFisher Scientific). Both strands of each product were sequenced using an ABI3100 capillary sequencer (MACROGEN Inc.), with the primers used for PCR. Finally, the chromatograms were visualized and aligned with BIOEDIT 7.0.5 (Hall, 1999).

Genetic variability and phylogenetic inference

We tested for incongruence of substitution rates of the combined dataset with the partition homogeneity test (Farris *et al.*, 1995), as implemented in PAUP* (Swofford, 1998). The result of this test showed that the sequence for the two loci were congruent ($P = 0.30$), and thus a concatenated fragment of mtDNA adding 1306 bp was used. We calculated several descriptors of genetic variability, including the number of variable sites (S), number of haplotypes (H), nucleotide diversity (π) and haplotype diversity (Hd) using ARLEQUIN 3.5 (Excoffier & Lischer, 2010).

We performed a Genetic Landscape Shape Interpolation analysis using the software ALLELES IN SPACE (Miller, 2005) to assess the existence of barriers to gene flow and areas of high genetic richness occurring in our dataset. We created two different connectivity networks: the pairwise location-based network and the Delaunay triangulation-based network. We chose a grid of 60 cells (east–west) × 120 cells (north–south) to represent the study area. The output was overlapped on a map of the area using DIVA-GIS v.7.5.0 (http://www.diva-gis.org/).

A Bayesian phylogenetic analysis was performed using BEAST 1.8.2 (Drummond *et al.*, 2012) for the concatenated dataset (*CR* + *NAD*). We ran the analysis using a relaxed uncorrelated molecular clock and HKY+G model of nucleotide substitution, chosen after running jModeltest (Posada, 2008). We used three calibration points obtained from Johnson *et al.* (2006): lineage ocelot of 2.91 Mya [95% highest posterior density (HPD): 2.02–4.25 Mya]; *Leopardus pardalis–Leopardus weidii*, 1.58 Mya (95% HPD: 1.01–1.24 Mya) and *Leopardus geoffroyi–Leopardus guigna*, 0.74 Mya (95% HPD: 0.41–1.21 Mya), with normal prior distribution and a Yule tree prior. The analysis was performed for 10^8 iterations and parameters were sampled every 10 000 iterations. Acceptable convergence to stationarity was checked using the program TRACER 1.7.0 (Rambaut *et al.*, 2018). A maximum credibility tree was summarized using TreeAnnotator 1.8.2 (Drummond *et al.*, 2012). The sequences of *L. pardalis* (Accession No. NC_028315.1) and *L. guigna* (Accession No. NC_028321.1) were included as outgroups. We also constructed maximum likelihood and parsimony trees with PAUP v.4.0 (Swofford, 1998). The best-fitting model of nucleotide substitution was selected with jModeltest as before. Maximum parsimony and maximum likelihood heuristic searches were conducted with 1000 random sequence addition replicates. Relationships among haplotypes were studied with a network constructed with TCS (Clement *et al.*, 2000) implemented in the software PopArt (http://popart.otago.ac.nz).

Finally, we calculated the fixation index Φ_{ST} using analysis of molecular variance (AMOVA) (Excoffier *et al.*, 1992) implemented in ARLEQUIN to evaluate the differentiation among groups detected with the previous analyses. The correlation between genetic and geographical distances was assessed with a Mantel test (Mantel, 1967) with 1000 permutations using the program ALLELES IN SPACE (Miller, 2005).

Demographic history

To analyse the demographic history of *L. geoffroyi*, we used two complementary approaches. First, and in order to estimate changes in population size over time, we constructed Bayesian skyline plots (BSPs) as implemented in BEAST 1.8.2 (Drummond *et al.*, 2012). The runs were performed for 5×10^7 iterations and parameters were sampled every 5000 iterations. We selected the most adequate nucleotide substitution model with jModeltest (Posada, 2008) and applied a relaxed molecular clock model with a mean rate of 0.0354 substitution/sites/Myr (SD = 0.000396) following the estimates of Trigo *et al.* (2013). We

ran two independent chains with identical settings, further combined into a single string, and discarding the 10% burn-in using the program LOG COMBINER 1.6.2 (Drummond & Rambaut, 2007). The results were visually inspected with the program TRACER 1.7.0 (Rambaut *et al.*, 2018). The effective sample size was used to assess the convergence of the strings with a threshold value of 200. In addition, we performed model comparisons (Constant size vs. BSP) within the Bayesian phylogenetic and phylogeographical analysis framework using the stepping-stone (SS) and path sampling (PS) marginal likelihood estimators (Xie *et al.*, 2011; Baele *et al.*, 2012) in BEAST.

Second, we used ARLEQUIN 3.0 (Excoffier *et al.*, 2005) to test for sudden demographic expansion using mismatch distribution analyses (Rogers & Harpending, 1992). We employed the sum of squared deviations (*SSD*) statistic and the raggedness index (*Rg*) defined by Harpending (1994) to test the goodness of fit of the observed mismatch distribution to that expected under the sudden expansion model. Additionally, to test for deviations from neutrality (as would be expected under demographic expansion) we used Fu's *F* (Fu, 1997) and *R2* (Ramos-Onsins & Rozas, 2002). The significance of these statistics was tested with DNAsp v.5 (Rozas & Rozas, 1995).

Ancestral distribution estimates

We used the continuous diffusion model implemented in BEAST (Lemey *et al.*, 2010) to estimate the patterns of ancestral distribution of the group. We ran the analysis with a smaller dataset, selecting only one individual representing each haplotype found in a given locality. We performed runs for each dispersal process (Homogeneous Brownian, Gamma, Cauchy and Lognormal) and compared them through a Marginal Likelihood Estimation analysis. The most appropriate model (Gamma RRW model) for the dataset was finally used for the phylogeographical analysis, with the same calibration points as before. The maximum clade credibility tree was obtained with TreeAnnotator 1.8.2 (Drummond *et al.*, 2012) and used as input in SPREAD3 (Bielejec *et al.*, 2016) to generate time-calibrated reconstruction of the diffusion process. Finally, we used TimeSlicer (kindly provided by P. Lemey) to summarize the variation in diffusion rate over time based on the posterior sample of trees at multiple time slices.

Species distribution models

To study the probable changes in the distribution of *L. geoffroyi* through time, we created SDMs using the maximum entropy method in MaxENT v.3.4.0 (Phillips *et al.*, 2017). Climatic variables for current and past conditions were downloaded from WorldClim (http://www.worldclim.org). We ran the distribution model for current conditions, and then projected onto palaeoclimatic models for the Last Interglacial period (LIG; 120 000–140 000 years BP) and for the LGM (22 000 years BP). Current and LIG models were run using the finer spatial resolution of 30 arc seconds, while the projections for the LGM were run at 2.5 arc minutes resolution. Past climatic models were taken from the Model for Interdisciplinary Research On Climate (MIROC) for the LGM and Otto-Bliesner *et al.* (2006) for the LGI. We also included three topographic variables (altitude, slope and aspect), derived from a digital elevation model produced by the NASA—Shuttle Radar Topographic Mission.

In addition to the 72 samples used in this work, we included 266 presence records reported by Cuyckens *et al.* (2016). We tested for correlation between environmental variables using Pearson's correlation coefficient (r) implemented in ENM Tools (Warren *et al.*, 2010; Warren & Seifert, 2011). For model calibration, we varied the regularization multiplier values following Anderson & Gonzales (2011). This parameter penalizes complex models that include many features and compel MaxENT to concentrate on only those with the highest explanatory capability (Phillips *et al.*, 2006). We tested 10 regularization values from 0.5 to 5. For each run we split the data as 75% (training data) and 25% (test data), for 10 replicates (run type = bootstrap) and 2500 maximum iterations. We evaluated the performance of the different values using Akaike's information criterion (AIC) using ENM Tools (Warren *et al.*, 2010; Warren & Seifert, 2011).

Based on the results of the calibration, we ran 10 different models including the one with all the variables and nine more combining non-correlated ($r < 0.8$) variables with >1% contribution to the model. We then evaluated model performance with the Model Selection tool in ENM Tools. Finally, we carried out model projections using the selected environmental variables and regularization value through the MESS analysis implemented in MaxENT.

RESULTS

Genetic variability

We sequenced 1306 bp in 72 individuals and identified 56 haplotypes (Supporting Information, Table S1). Only 10 haplotypes were shared between individuals. There were 85 variable sites, 47 of which were phylogenetically informative. Nucleotide diversity (π) was 0.09, haplotypic diversity 0.982 and mean pairwise difference 8.920.

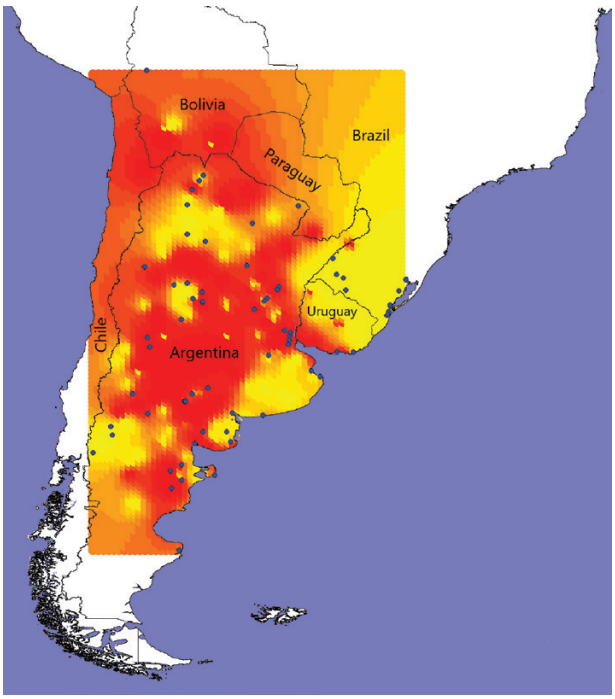

Figure 2. Landscape Genetic Shape Interpolation obtained from all individuals, according to the Delaunay triangulation. Yellow: low levels of genetic difference between individuals. Red: high levels of genetic difference between individuals. Blue dots represent collection points.

Figure 2 shows the results of the Genetic Landscape Shape Interpolation according to the Delaunay triangulation (the pairwise location-based network was essentially the same). The map reveals higher genetic diversity at the centre of the distribution, with some small areas of low diversity embedded within it. The peripheral part of the distribution, especially the region in Brazil and Uruguay, shows lower diversity than the centre.

Phylogenetic analyses

The phylogenetic trees constructed using Bayesian inference, maximum likelihood and parsimony were consistent in their main topology. Therefore, we only show the Bayesian tree constructed with BEAST (Fig. 3). All haplotypes corresponding to *L. geoffroyi* were grouped into a monophyletic cluster with maximum posterior probability. As suggested by other studies (Johnson *et al.*, 1999, 2006), *L. guigna* is confirmed as the sister species of Geoffroy's cat. The estimated time to the most recent common ancestor (TMRCA) for the species is 0.78 Mya (95% HPD 0.47–1.14 Mya).

The topology of the tree indicates two moderately supported clades (0.5 and 0.7 posterior probability). The estimated TMRCAs for the two clades were 0.64 Mya (95% HPD = 0.35–0.98 Mya) and 0.59 Mya (95% HPD = 0.32–0.94 Mya) respectively. A close examination to the geographical origin of samples within each clade (Fig. 1) shows no evident geographical pattern or relationship with the four subspecies described for *L. geoffroyi*. However, again there appears to be a central/marginal pattern, as indicated by the variable levels of genetic diversity analysed earlier: the central clade (C) is slightly older than the peripheral one (P). This younger clade includes all samples from Bolivia, Brazil and Uruguay, while the older clade comprises only Argentinian samples.

The haplotypic network (Fig. 4) showed similar geographical structure to the one observed in the phylogenetic trees. In this case, each clade (Central and Peripheral) appears subdivided, with no evident geographical correlation. When comparing both C and P clades using AMOVA, there were significant differences (Φ_{ST} = 0.397, $P < 0.001$). Mantel tests within each clade did not show any correlation between geographical and genetic distances.

Demographic history

The mismatch distribution analysis for the entire dataset resulted in a unimodal distribution with mode around 13 pairwise differences. Fu's *F* and *R2* were also significant, indicating expansion [Fu's $F = -0.364$, $P < 0.005$; $R2 = 0.097$ (95% confidence interval 0.047–0.159), $P < 0.05$]. The sum of squared deviation (*SSD*) and raggedness index (*Rg*) statistics showed demographic expansion (*SSD* = 0.00047, $P = 0.99$; *Rg* = 0.0023, $P = 0.97$) as well as spatial expansion (*SSD* = 0.0017, $P = 0.61$; *Rg* = 0.0023, $P = 0.97$). Each individual clade showed also a demographic history of expansion. The TMRCA was 0.44 Mya for the Central clade and 0.37 Mya for the Peripheral clade.

The BSP combined with the plot for dispersal rate through time (Fig. 5) revealed two periods of population growth in effective size. The first one would have begun ~190–170 kya, producing a 10-fold increase in effective size. After a period of relative stability, a second growth accompanied by an increase of dispersal rate, i.e. population and geographical expansions, occurred at ~45–35 kya, also resulting in a 10-fold increase in effective size. Thus, the final mean population size was 100 times higher than before the two expansions.

Diffusion analysis

The spatial diffusion rate for the group was 2058 km/Myr (95% HPD = 1524–2634 km/Myr), roughly 2 m/year. The model inferred that the expansion of the species would have begun at ~500 kya, near the time of the previously suggested origin of the two clades found

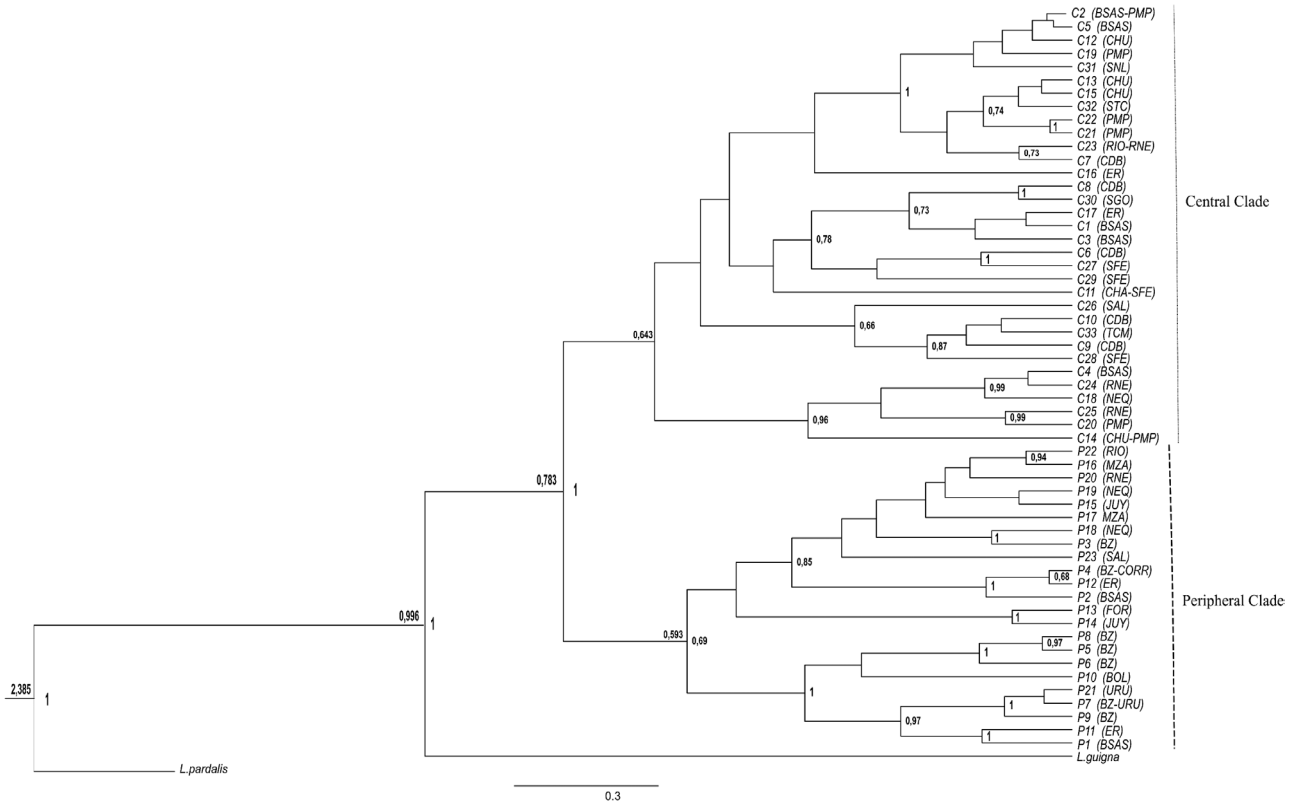

Figure 3. Maximum credibility tree of *Leopardus* geoffroyi from mtDNA reconstructed using Bayesian inference. Posterior probabilities >0.5 are indicated to the right of the nodes. Numbers to the left of each node are the estimated divergence times in million years. C1 to C33: haplotypes belonging to the Central Clade, P1 to P23, haplotypes of the Peripheral Clade. Sample names indicate geographical areas as in Figure 1. Scale bar in mean number of substitutions per million years.

in the phylogenetic analysis. The model also located its geographical origin in Central Argentina (Fig. 6A), from where the lineage diversification started towards the north and the south (Fig. 6B). The spatio-temporal reconstruction of the diversification indicates further expansions in the same directions, along with expansions to the east and west between 300 and 150 kya, colonizing Paraguay, Bolivia, Uruguay, Brazil and the Andes (Fig. 6C, D). In particular, the LIG expansions (between 150 and 120 kya) showed the advance towards the south of Brazil and Bolivia (Fig. 6E). The last and highest lineage diversification, during the LGM (~20 kya), arrived in the previously unoccupied Patagonia in Argentina and Chile (Fig. 6F).

Species distribution model

Based on Pearson's correlations and contributions to the full model, we selected eight of the 19 bioclimatic variables producing three models with different combinations of non-correlated variables (Supporting Information, Table S2). Area under the curve (AUC) values between models were similar and >0.8. The most accurate model according to the AIC is shown in Figure 7 and Table S2. The bioclimatic variables that contributed the most to the selected model were Temperature Seasonality (Bio04), followed by Precipitation of Wettest Month (Bio13), Min. Temperature of Coldest Month (Bio06), Precipitation of Driest Quarter (Bio17) and Precipitation Seasonality (Bio15).

The palaeo-distribution obtained during the LIG (120 kya) shows a very sharp limit among good/very good and poor niche conditions for the presence of the species, following an especially dry subtropical region of the Andes known as the 'dry diagonal'. South of this diagonal, the probability of occurrence of the species is very low. Conversely, a high probability of occurrence is predicted north of the diagonal, where the diffusion analysis inferred the origin and initial expansion of the lineage.

The model for the LGM (21 kya) showed a reduction of high-probability areas, as well as total presence areas, which are restricted to the north of 37°S. The probability of presence to the west, where the elevation is increasingly higher, is similar to that shown by the LIG model.

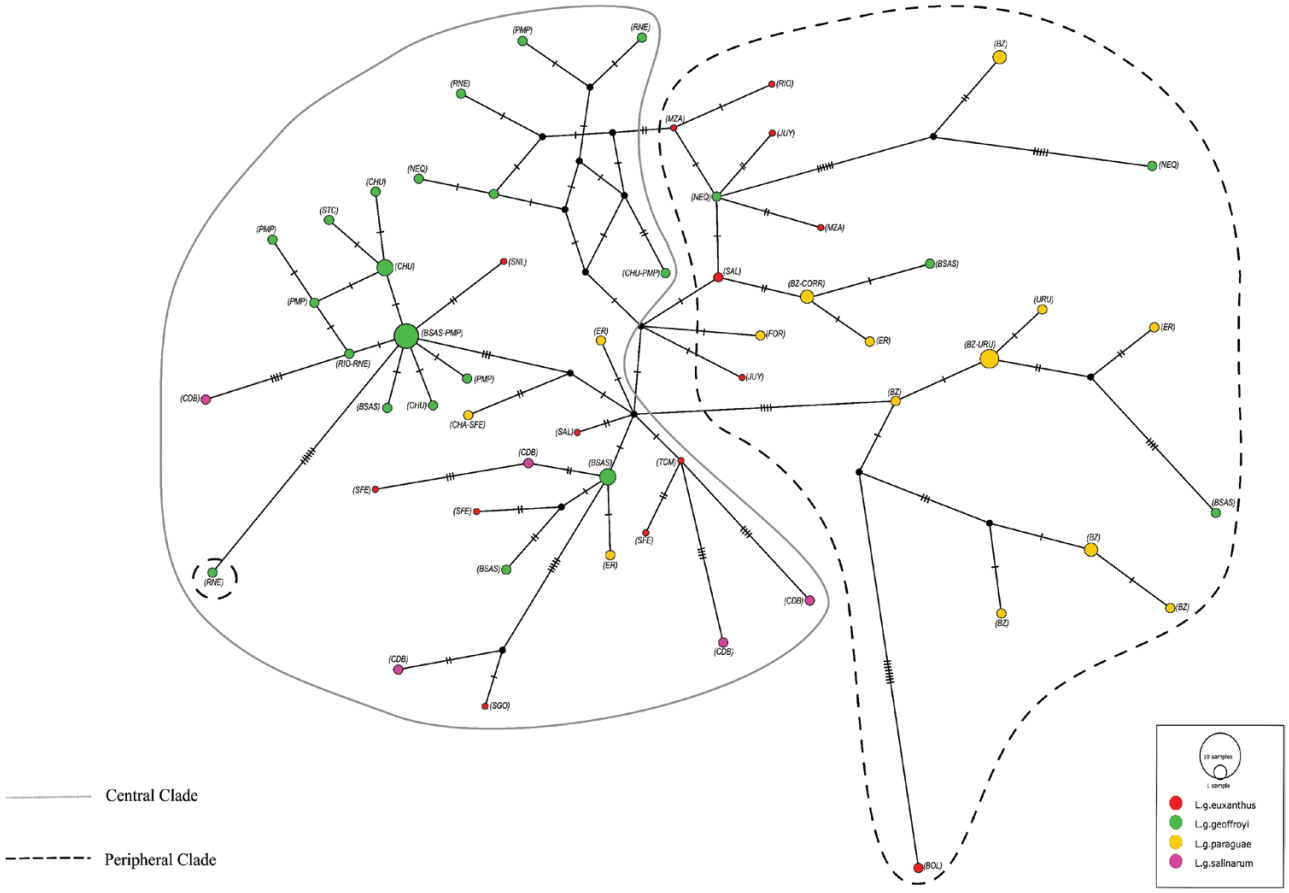

Figure 4. Haplotypic network based on mtDNA in *Leopardus* geoff*royi*. Haplotypes are represented by circles, the size of which is proportional to their frequency. Lines on branches indicate the number of mutational steps separating haplotypes; colours indicate previously proposed subspecies. Lines encircle Central and Peripheral Clades. Names of the geographic areas, as in Figure 1, are given in parentheses.

The distribution model for the present climatic conditions showed a similar distribution to the LIG model, with some differences. First, and importantly, the area south to the dry diagonal now has higher probabilities of occurrence, especially the coastal zone of Patagonia. Second, the areas with the highest probabilities of presence are located at the eastern and northern edges of the distribution range, including coastal areas of eastern Argentina, Uruguay, South Brazil and Paraguay. Third, favourable areas diminished in the Gran Chaco and Cerrado in Bolivia.

DISCUSSION

How many, if any, subspecies?

The Ocelot lineage is one of the two lineages of felids living in South America. It diversified between 8 and 2.9 Mya, after the faunal exchange between North and South America facilitated by the emergence of the Panamanian land bridge (Johnson *et al.*, 2006). The lineage includes eight *Leopardus* species: *L. pardalis*, *L. weidii*, *L. jacobita*, *L. colocola*, *L. tigrinus*, *L. guigna*, *L. guttulus* and *L. geoffroyi*. The taxonomy and genetics of most of these species have been studied in depth; however, that is not the case for *L. geoffroyi*. Therefore, we present here the first exhaustive (regarding sampling and geography) study of the genetic variability, genetic structure and intraspecific taxonomic status of *L. geoffroyi*. We also show results that help to elucidate the demographic history of the species.

Based on samples collected in the wild from all four putative subspecies of *L. geoffroyi*, we found no phylogenetic evidence supporting any subdivision of the species. Furthermore, we detected two clades congruent with the spatial diffusion model we obtained, but completely dissimilar to the geographical range of the four described subspecies. Given that the morphological data (Nascimento, 2014) also do not appear to support the subspecies distinction, we are proposing to accept *L. geoffroyi* as a monotypic

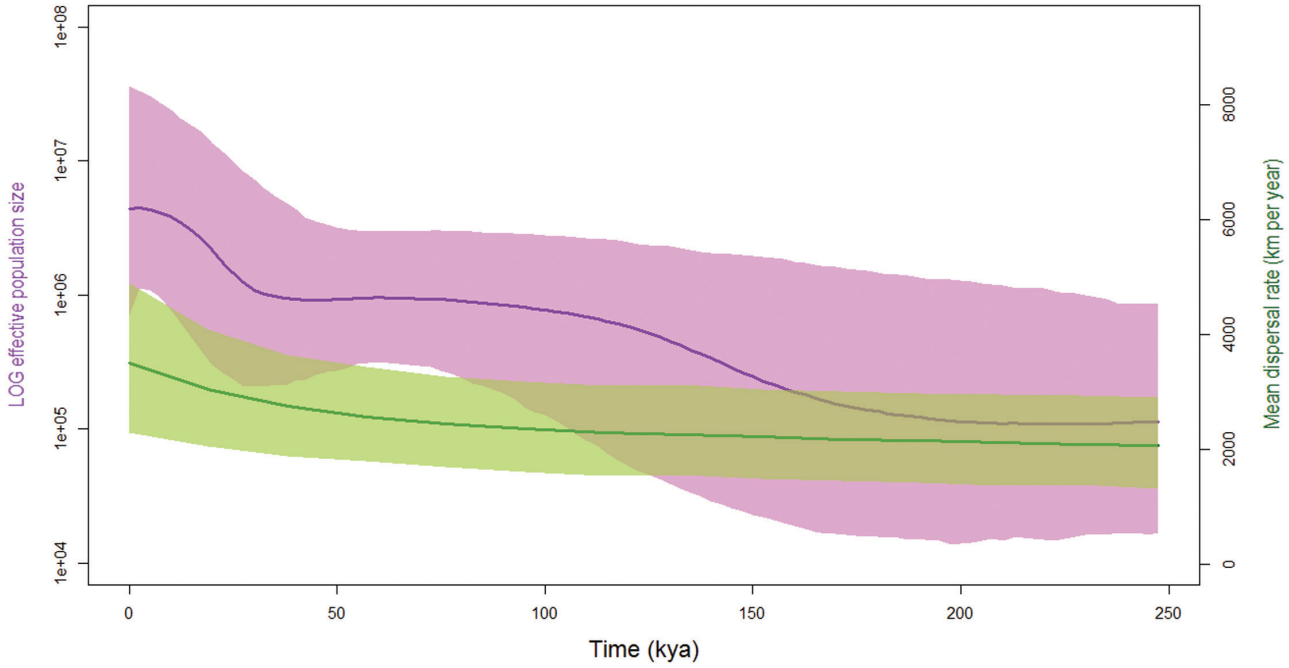

Figure 5. Variation through time in effective population size and dispersal rate in *Leopardus geoffroyi* based on a Bayesian Skyline Plot. The right *y*-axis indicates the rate of dispersal per million years expressed in km per year (green), and the left *y*-axis the effective population size expressed on a logarithmic scale (pink). Bold lines give the median of each estimation, while the 95% highest posterior densities are indicated by the shaded areas.

species. The only previous phylogeographical study on the species, performed based on samples from captive individuals (whose geographical origin certainty depends on the zoo's records) also supported this taxonomic arrangement (Johnson *et al.*, 1999).

Genetic variability and demographic history

The criteria used by the IUCN to categorize species in the Red List include small and fragmented populations, suffering or having suffered population decline. Translating these criteria to genetic terms means considering the effects of genetic drift and therefore low genetic diversity. The Ocelot lineage comprises species in all four IUCN Red List categories, with haplotype diversity between 0.46 and 0.98, and nucleotide diversity varying by more than one order of magnitude, from 0.0030 to 0.098 (see references in the next paragraph).

The most threatened species in the lineage, *L. jacobita*, has the lowest level of variation ($\pi = 0.0030$, $H = 0.46$, Ruiz García *et al.*, 2013). We found that *L. geoffroyi*, categorized as LC according to the IUCN, has a nucleotide diversity of 0.090 and a haplotype diversity of 0.98. These values are similar to those found in the margay, *L. weidii* (Eizirik *et al.*, 1998), species NT according to the IUCN Red List, and half of that of the kodkod (*L. guigna*: Johnson *et al.*, 1999; Napolitano *et al.*, 2012), its sister species and categorized as Vulnerable. The remaining species of the group have intermediate levels of variability, regardless of their conservation status. Johnson *et al.* (1999) reported for Geoffroy's cat a nucleotide diversity of 0.027, three times lower than the one found here. We believe that this difference lies in the fact that all samples used in Johnson's study came from captive individuals, where inbreeding is quite common (Frankham *et al.*, 2010).

The low magnitude of the nucleotide diversity associated with high haplotype diversity indicates a pattern of recent and rapid expansion, consisting of many haplotypes differentiated by only a few mutations. This pattern is also found in other species of the group such as *L. colacola* (Cossios *et al.*, 2009; Santos *et al.*, 2018) and *L. guigna* (Napolitano *et al.*, 2014). The geographical distribution of this genetic variability is not clinal, as suggested by morphology (Nascimento, 2014), but rather is arranged in a central–peripheral pattern where the highest variability is located at the centre (Fig. 2). Theory predicts that the geographical origin of a lineage will show the highest genetic diversity, which would be reduced as its expansion occurs, being lowest at the edges of the distributional range (Eckert *et al.*, 2008). Therefore, the geographical distribution of genetic variability found in our work suggests an origin of the species in Central Argentina, a result also shown by the phylogenetic reconstruction (Fig. 3) and the spatial diffusion model (Fig. 6).

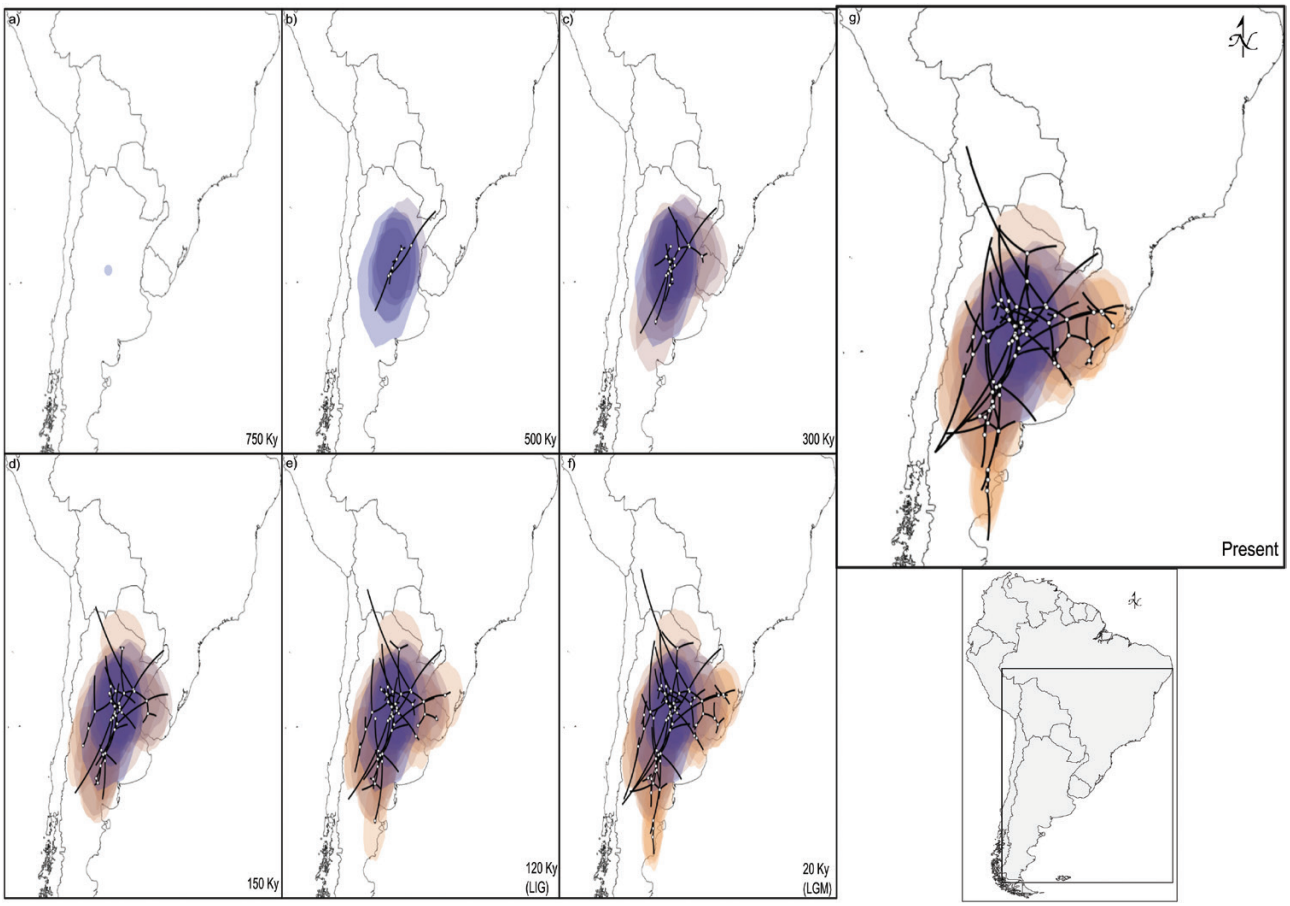

Figure 6. Spatial projection of the diffusion pattern through time, based on the maximum clade credibility (MCC) tree, estimated by Bayesian phylogeographical analysis in BEAST at the times indicated at the bottom of each panel. The lines represent the branches of the MCC tree; coloured areas represent the 80% highest posterior density uncertainty in the location of ancestral branches with a gradient from dark to light representing older to younger diffusion events. Purple indicates the central clade, while pink indicates the peripheral clade.

The haplotype network does not show any evident expansion: there are no widespread haplotypes (the most frequent one was found seven times, most of the haplotypes being represented only once), and most of the branches connecting them have between two and five nucleotide differences. Despite the network resembling a pattern of population stability, the mismatch analysis, Fu's *F* and *R2* showed signals of demographic expansion. However, these analyses are shown to be effective only in cases of recent expansions and they fail to distinguish between demographic (It is now possible to discriminate between the two situations using Bayesian phylogeographical inference and SDMs (Lemey *et al.*, 2009, 2010; Camargo *et al.*, 2013; Baranzelli *et al.*, 2017). We are aware of the limitations of using only mtDNA to reconstruct demographic history, but different lines of evidence produced concordant results, as detailed below.

We found that the separation between *L. geoffroyi* and its sister species, *L. guigna*, occurred ~783 000 years ago (Fig. 3), similar to the divergence time estimated with mitogenomics for both species (0.68–0.52 Mya: Ruiz-García *et al.*, 2017). The origin of the species is located in Central Argentina (Fig. 6A). From this geographical origin, the Central Clade originated ~640 000 years ago and diversified 200 000 years later (Fig. 6B). The Peripheral Clade arose from the central part of the distribution 590 000 years ago (Fig. 6B), starting its diversification 370 000 years ago (Fig. 6C). In Figure 6 we found a possible explanation for the existence of these two non-clinal clades, since the diffusion model shows long branches leading to the north and the south – the Peripheral Clade – as well as more nodes and shorter branches around the origin representing the Central Clade. The diversification of both clades seems to continue to the present.

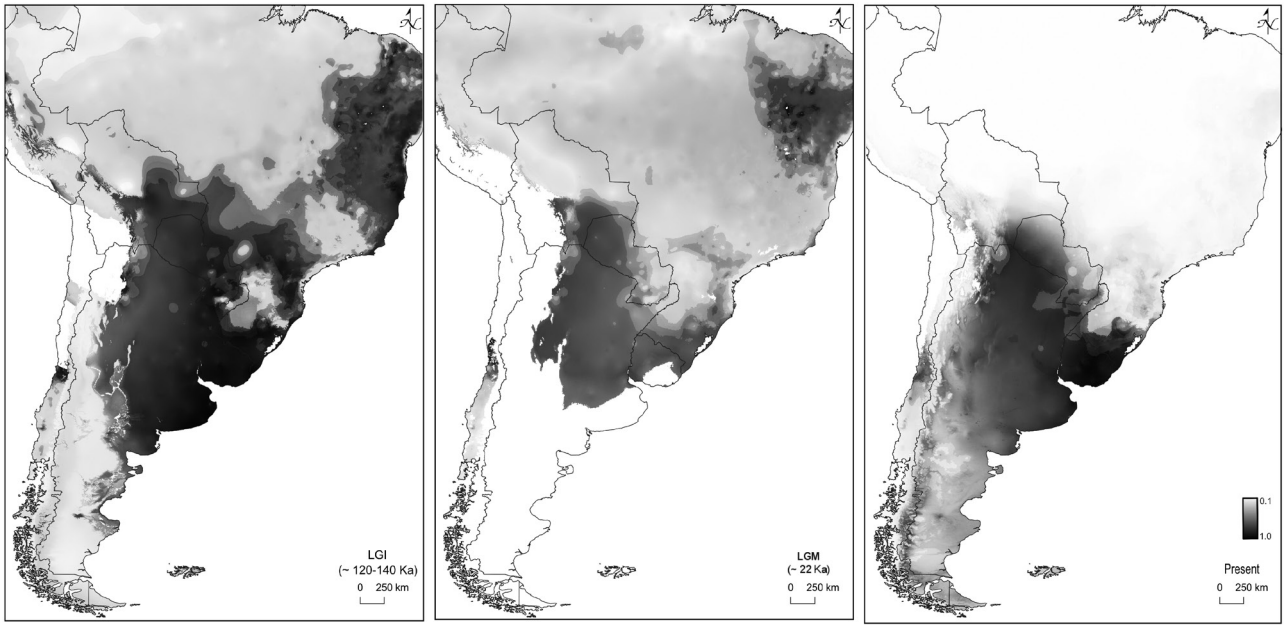

Figure 7. Changes in the potential distribution of *Leopardus geoffroyi*. Potential distributions are shown in grey; darker shading indicates areas that are more favourable during the Last Interglacial Maximum (LIG), Last Glacial Maximum (LGM) and present times.

Late Pleistocene demographic history and palaeo-distribution modelling

Climate change produced shifts of the different biomes. Sea level fell during glacial periods, and in the southern part of South America, the submarine platform became partially exposed, from 10 to 140 m during full glacial periods. There was an increase in extreme temperatures as well as reduction in precipitation, mainly in the Pampas and Patagonia, from approximately 34°S to the south. These glacial episodes led to the formation of sand dunes in these regions. Regarding vegetation cover, displacement of the forest led to shrubby steppe environments. In addition, the grassland was reduced, replaced by the monte and steppe ecosystems (Rabassa *et al.*, 2005).

Our results show the origin of *L. geoffroyi* in central Argentina, the current Espinal biome (thorny deciduous shrubland forests), during the Pleistocene around 758 000 years ago. The species shows very high ecological plasticity, living in a broad array of natural habitat types, including scrublands, dry forests, savannas, grasslands, marshlands and steppes of the subtropical and temperate Neotropics (Cuyckens *et al.*, 2016). This ecological plasticity constitutes an obvious advantage during climate change. Although the existence of stable areas, i.e. refugia, during the glaciations in South America has been described only for Patagonia (Sersic *et al.*, 2011), it is safe to assume that in more temperate zones, like the Espinal, the Pampas and the Monte biomes, they must have existed as well. Moreover, for species associated with open vegetation, such as Geoffroy's cat, previous study indicates that during glacial periods they could have shrunk, maintained or even expanded their geographical ranges (Turchetto-Zolet *et al.*, 2013).

According to the Skyline plot analyses (Fig. 5), a high rate of increase in effective number without range expansion occurred for *L. geoffroyi* before the LIG, starting ~170 000 years ago. Bayesian diffusion analysis (Fig. 6) shows that the lineage then extended its range northwards, reaching Paraguay, and southwards to the Monte-Desert and Patagonian Steppe ecoregions. This range expansion is shown as a slightly but continuous increase in the curve of the Skyline plot. After the LGM, there is a period of stability in effective population size (*Ne*).

Strong evidence of population growth combined with range expansion through time was obtained during the LIG approaching the LGM. Spatio-temporal reconstruction indicated that such an expansion would have started ~40 000 years ago, during the LIG, and lasted until the beginning of the LGM. The resulting *Ne* was ~100 times higher after the two expansions. Diffusion analysis shows that around this time, the species extended its range further north to Bolivia and south to coastal Patagonia. At this time, the species crosses the Dry Diagonal, a transition zone between two circulation systems found in South America that influences the climate. The Dry Diagonal has been

shown to be a clear divisor between 'good' and 'poor' niches for many species (Bruniard, 1982). However, it does not seem to have acted as a barrier either for Geoffroy's cat or for *L. colocola* (Santos *et al.*, 2018), which show central/peripheral and west/east differentiation, respectively.

Leopardus colocola also suffered two episodes of population expansion at approximately the same geological time as Geoffroy's cat (Santos *et al.*, 2018), 200 and 60–50 kya, the latter period coinciding with the expansion of the savanna in Brazil. *Leopardus geoffroyi* populations expanded 180 000 and 40 000 years ago, being the late Pleistocene expansion coincident with the advance of the Monte vegetation to the north (Baranzelli *et al.*, 2017). However, a very important difference exists between these two felid species: while *L. colocola* has a genetic structure indicating four subspecies with distributions historically linked to glacial episodes, we found that *L. geoffroyi* constitutes a monotypic species distributed in many different biomes. Moreover, we found that late glaciations had little or no effect on the demographic expansions that occurred during the LIG, as shown in other vertebrates such as lizards (Olave *et al.*, 2011; Camargo *et al.*, 2013), fish (Ruzzante *et al.*, 2008) and rodents (Lessa *et al.*, 2010).

The SDM based on climatic variables shows that during the LIG, a large portion of South America was suitable for the species. After the LGM the distribution shifted southwards, and the whole region of Patagonia became habitat with different degrees of suitability for the species. The range expansion to the south that started before the LGM (Figs 5, 6E) probably continued after the glaciation, without significant retreat, and resulted in the presence of this felid in the far south of Patagonia. Thus, our comparisons using independent approaches such as SDM and Bayesian reconstruction of the diffusion process agreed in the spatial direction of the range expansion.

This study is the first to include samples of Geoffroy's cat collected in the field from its entire distribution. We show that it is a monotypic species with one of the highest levels of genetic variability within the Ocelot lineage and demonstrate through different lines of evidence its evolutionary history of demographic and spatial expansions. These results, in agreement with other phylogeographical studies of co-distributed species, will fill an important gap in the knowledge of the effect of glacial cycles in the Southern Hemisphere. They will also contribute to the conservation of this species in highlighting the existence of a unique evolutionary significant unit.

ACKNOWLEDGEMENTS

We thank T. C. Trigo, A. Abba, G. Aprile, M. Carrera, S. de Bustos, A. Di Giácomo, N. Fracassi, J. Liotta, M. Monteverde, M. Morales, R. Palacios, H. Pastore, A. Paviolo, N. Pelegrin, V. Raimondi, M. Superina and A. Ximenez for providing samples. We also thank Museo Argentino de Ciencias Naturales 'Bernardino Rivadavia' (D. Flores), Colección Boliviana de Fauna (I. Moya), Museo de La Plata (M. Merino), Colección de Mamíferos de la Fundación Azara (Y. Davies) and Grupo de Ecología Comportamental de Mamíferos (E. Casanave and M. Lucherini) for allowing us access to samples in their collections. We also thank four anonymous reviewers for their insightful comments. Funding was provided by FONCyT (PICT 2016-4087), CONICET (PIP 114-201101-00050), Amersfoort Zoo, Feline Conservation Federation and Le Parc des Felines.

REFERENCES

Anderson RP, **Gonzales I Jr**. **2011.** Species-specific tuning increases robustness to sampling bias in models of species distributions: an implementation with Maxent. *Ecological Modelling* **222:** 2796–2811.

Baele G, **Lemey P**, **Bedford T**, **Rambaut A**, **Suchard MA**, **Alekseyenko AV. 2012.** Improving the accuracy of demographic and molecular clock model comparison while accommodating phylogenetic uncertainty. *Molecular Biology and Evolution* **29:** 2157–2167.

Baranzelli MC, **Cosacov A**, **Ferreiro G**, **Johnson L**, **Sérsic AN. 2017.** Travelling to the south: phylogeographic spatial diffusion model in *Monttea aphylla* (Plantaginaceae), an endemic plant of the Monte Desert. *PLoS ONE* **12:** 0178827

Bielejec F, **Baele G**, **Vrancken B**, **Suchard MA**, **Rambaut A**, **Lemey P. 2016.** Spread3: interactive visualization of spatiotemporal history and trait evolutionary processes. *Molecular Biology and Evolution* **33:** 2167–2169.

Bruniard ED. 1982. La diagonal árida argentina: un límite climático real. *Revista Geográfica* **95:** 5–20.

Cabrera A. 1958. Catálogo de los Mamíferos de América del Sur. *Revista del Museo Argentino de Ciencias Naturales* **4:** 1–307.

Camargo A, **Werneck F**, **Morando M**, **Sites JW Jr**, **Avila L. 2013.** Quaternary range and demographic expansion of *Liolaemus darwinii* (Squamata: Liolaemidae) in the Monte Desert of Central Argentina using Bayesian phylogeography and ecological niche modelling. *Molecular Ecology* **22:** 4038–4054.

Clapperton CM. 1993. *Quaternary geology and geomorphology of South America*. New York: Elsevier.

Clement M, **Posada D**, **Crandall K. 2000.** TCS: a computer program to estimate gene genealogies. *Molecular Ecology* **9:** 1657–1659.

Cosacov Martinez A, **Sersic AN**, **Sosa V**, **Johnson LA**, **Cocucci AA. 2010.** Multiple periglacial refugia in the Patagonian steppe and post-glacial colonization of the Andes: the phylogeography of *Calceolaria polyrhiza*. *Journal of Biogeography* **37:** 1463–1477.

Cossíos D, **Lucherini M**, **Ruiz-García M**, **Angers B. 2009.** Influence of ancient glacial periods on the Andean fauna: the case of the pampas cat (*Leopardus colocolo*). *BMC Evolutionary Biology* **9:** 68.

Cuyckens GAE, **Pereira JA**, **Trigo TC**, **Da Silva M**, **Goncálves L**, **Huaranca JC**, **Bou Pérez N**, **Cartes L**, **Eizirik E. 2016.** Refined assessment of the geographic distribution of Geoffroy's cat (*Leopardus geoffroyi*) (Mammalia: Felidae) in the Neotropics. *Journal of Zoology* **298:** 285–292.

Drummond AJ, **Rambaut A. 2007.** BEAST: Bayesian Evolutionary Analysis Sampling Trees. *BMC Evolutionary Biology* **7:** 214.

Drummond AJ, **Suchard MA**, **Xie D**, **Rambaut A. 2012.** Bayesian phylogenetics with BEAUti and the BEAST 1.7. *Molecular Biology and Evolution* **29:** 1969–1973.

Eckert CG, **Samis KE**, **Lougheed SC. 2008.** Genetic variation across species' geographical ranges: the central–marginal hypothesis and beyond. *Molecular Ecology* **17:** 1170–1188.

Eizirik E, **Bonatto SL**, **Johnson WE**, **Crawshaw PG**, **Vié JC**, **Brousset DM**, **O´Brien SJ**, **Salzano FM. 1998.** Phylogeographic patterns and evolution of the mitochondrial DNA control region in two neotropical cats (Mammalia, Felidae). *Journal of Molecular Evolution* **47:** 613–624.

Elith J, **Kearney M**, **Phillips S. 2010.** The art of modelling range-shifting species. *Methods in Ecology and Evolution* **1:** 330–342.

Elith J, **Leathwick JR. 2009.** Species distribution models: ecological explanation and prediction across space and time. *Annual Review of Ecology, Evolution and Systematics* **40:** 677–697.

Excoffier L, **Laval LG**, **Schneider S. 2005.** Arlequin ver. 3.0: an integrated software package for population genetics data analysis. *Evolutionary Bioinformatics Online* **1:** 47–50.

Excoffier L, **Lischer HEL. 2010.** Arlequin Suite ver. 3.5, a new series of programs to perform population genetics analyses under Linux and Windows. *Molecular Ecology Resources* **10:** 564–567.

Excoffier L, **Smouse PE**, **Quattro JM. 1992.** Analysis of molecular variance inferred from metric distances among DNA haplotypes: application to human mitochondrial DNA restriction data. *Genetics* **131:** 479–491.

Farris JS. Källersjö M, **Kluge AG**, **Bult C. 1995.** Testing significance of incongruence. *Cladistics* **10:** 315–319.

Frankham R, **Ballou JD**, **Briscoe DA. 2010.** *Introduction to conservation genetics*. Cambridge: Cambridge University Press.

Fu Y. 1997. Statistical tests of neutrality of mutations against population growth, hitchhiking and background selection. *Genetics* **147:** 915–925.

Hall T. 1999. BioEdit: a user-friendly biological sequence alignment editor and analysis program for Windows 95/98/NT. *Nucleic Acids Symposium Series* **41:** 95–98.

Harpending RC. 1994. Signature of ancient population growth in a low-resolution mitochondrial DNA mismatch distribution. *Human Biology* **66:** 591–600.

Hewitt GM. 2000. The genetic legacy of the Quaternary ice ages. *Nature* **405:** 907–913.

Hewitt GM. 2004. The structure of biodiversity—insights from molecular phylogeography. *Frontiers in Zoology* **1:** 4–20.

Johnson WE, **Pecon-Slattery J**, **Eizirik E**, **Kim J-H**, **Menotti-Raymond M**, **Bonacic C**, **Cambre R**, **Crawshaw P**, **Nunez A**, **Seuánez HN**, **Martins Moreira MA**, **Seymour KL**, **Faiçal S**, **Swanson W**, **O'Brien SJ. 1999.** Disparate phylogeographic patterns of molecular genetic variation in four closely related South American small cat species. *Molecular Ecology* **8:** 79–94.

Johnson WE, **Eizirik E**, **Pecon-Slattery J**, **Murphy WJ**, **Antunes A**, **Teeling E**, **O'Brien SJ. 2006.** The late Miocene radiation of modern Felidae: a genetic assessment. *Science* **311:** 73–77.

Kitchener AC, **Breitenmoser-Wursten Ch**, **Eizirik E**, **Gentry A**, **Werdelin L**, **Wilting A**, **Yamaguchi N**, **Abramov AV**, **Christiansen P**, **Driscoll C**, **Duckworth JW**, **Johnson W**, **Luo SJ**, **Meijaard E**, **O'Donoghue P**, **Sanderson J**, **Seymour K**, **Bruford M**, **Groves C**, **Hoffmann M**, **Nowell K**, **Timmons Z**, **Tobe S. 2017.** A revised taxonomy of the Felidae. The final report of the Cat Classification Task Force of the IUCN/SSC Cat Specialist Group. *Cat News Special Issue* **11:** 80.

Knowles L, **Carstens BC. 2007.** Delimiting species without monophyletic gene trees. *Systematic Biology* **56:** 887–895.

Kocher T, **Thomas W**, **Meyer A**, **Edwards S**, **Paabo S**, **Villablanca F**, **Wilson A. 1989.** Dynamics of mitochondrial DNA evolution in animals: amplification and sequencing with conserved primers. *Proceedings of the National Academy of Sciences USA* **86:** 6196–6200.

Lemey P, **Rambaut A**, **Welch JJ**, **Suchard MA. 2010.** Phylogeography takes a relaxed random walk in continuous space and time. *Molecular Biology and Evolution* **27:** 1877–1885.

Lemey P, **Suchard M**, **Rambaut A. 2009.** Reconstructing the initial global spread of a human influenza pandemic: a Bayesian spatial-temporal model for the global spread of H1N1pdm. *PLoS Currents* **1:** RRN1031.

Lessa EP, **D'Elía G**, **Pardiñas UFJ. 2010.** Genetic footprints of late Quaternary climate change in the diversity of Patagonian–Fueguian rodents. *Molecular Ecology* **19:** 3031–3037.

Mantel N. 1967. The detection of disease clustering and a generalized regression approach. *Cancer Research* **27:** 209–220.

Miller MP. 2005. Alleles in space: computer software for the joint analysis of interindividual spatial and genetic information. *Journal of Heredity* **96:** 722–724.

Miller SA, **Dykes DD**, **Polesky HF. 1988.** A simple salting out procedure for extracting DNA from human nucleated cells. *Nucleic Acids Research* **16:** 1215.

Napolitano C, **Johnson WE**, **Sanderson J**, **O'Brien SJ**, **Hoelzel AR**, **Freer R**, **Dunstone N**, **Ritland K**, **Ritland CE**, **Poulin E. 2014.** Phylogeography and population history of *Leopardus guigna*, the smallest American felid. *Conservation Genetics* **15:** 631–653.

Napolitano C, **Sanderson J**, **Johnson WE**, **O'Brien SJ**, **Hoelzel AR**, **Freer R**, **Dunstone N**, **Ritland K**, **Poulin E.**

2012. Population genetics of the felid *Leopardus guigna* in South America: identifying intraspecific units for conservation. In: Ruiz-García M, Shostell J, eds. *Molecular population genetics, phylogenetics, evolutionary biology and conservation of the Neotropical carnivores*. Hauppauge: Nova Science Publishers, 1–30.

Nascimento FO. 2014. On the morphological variation and taxonomy of the Geoffroy's cat *Leopardus geoffroyi* (d'Orbigny & Gervais, 1844) (Carnivora, Felidae). *Papéis Avulsos de Zoologia* **54:** 129–160.

Nascimento FO, **Feijó A. 2017.** Taxonomic revision of the tigrina *Leopardus tigrinus* (Schreber, 1775) species group (Carnivora, Felidae). *Papéis Avulsos de Zoologia* **57:** 231–264.

Olave M, **Martinez LE**, **Avila LJ**, **Sites JW**, **Morando M. 2011.** Evidence of hybridization in the Argentinean lizards *Liolaemus gracilis* and *Liolaemus bibronii* (Iguania: Liolaemini): an integrative approach based on genes and morphology. *Molecular Phylogenetics and Evolution* **61:** 381–391.

Otto-Bliesner BL, **Marshall SJ**, **Overpeck JT**, **Miller GH**, **Hu A. 2006.** Simulating Arctic climate warmth and icefield retreat in the Last Interglaciation. *Science* **311:** 1751–1753.

Pereira J, **Lucherini M**, **Trigo T. 2015.** *Leopardus geoffroyi. The IUCN Red List of Threatened Species 2015*, e.T15310A50657011. Available at https://www.iucnredlist.org/

Phillips SJ, **Anderson RP**, **Schapire RE. 2006.** Maximum entropy modeling of species geographic distributions. *Ecological Modeling* **190:** 231–259.

Phillips J, **Anderson RP**, **Dudík M**, **Schapire RE**, **Blair ME. 2017.** Opening the black box: an open-source release of Maxent. *Ecography* **40:** 887–893.

Pocock RI. 1940. The races of Geoffroy's cat (*Oncifelis geoffroyi*). *Annals and Magazine of Natural History* **6:** 350–355.

Posada D. 2008. jModelTest: phylogenetic model averaging. *Molecular Biology and Evolution* **25:** 1253–1256.

Rabassa J, **Coronato A**, **Bujalesky G**, **Salemme M**, **Roig C**, **Meglioli A**, **Heusser C**, **Gordillo S**, **Roig F**, **Borromei A**, **Quattrocchio M. 2000.** Quaternary of Tierra del Fuego, southernmost South America: an updated review. *Quaternary International* **68a:** 217–240.

Rabassa J, **Coronato AM**, **Salemme M. 2005.** Chronology of the Late Cenozoic Patagonian glaciations and their correlations with biostratigraphic units of the Pampan region (Argentina). *Journal of South American Earth Sciences* **20:** 81–103.

Rambaut A, **Drummond AJ**, **Xie D**, **Baele G**, **Suchard MA. 2018.** Posterior summarisation in Bayesian phylogenetics using Tracer 1.7. *Systematic Biology* **67:** 901–904.

Ramos-Onsins SE, **Rozas J. 2002.** Statistical properties of new neutrality tests against population growth. *Molecular Biology and Evolution* **19:** 2092–2100.

Rogers AR, **Harpending H. 1992.** Population growth makes waves in the distribution of pairwise genetic differences. *Molecular Biology and Evolution* **9:** 552–569.

Rozas J, **Rozas R. 1995.** DnaSP, DNA sequence polymorphism: an interactive program for estimating population genetics parameters from DNA sequence data. *Computer Applications in the Biosciences* **11:** 621–625.

Ruiz-García M, **Cossíos D**, **Lucherini M**, **Yáñez J**, **Pinedo-Castro M**, **Angers B. 2013.** Population genetics and spatial structure in two Andean cats (the Pampas cat, *Leopardus pajeros*, and the Andean mountain cat, *L. jacobita*) by means of nuclear and mitochondrial markers and some notes on skull biometrics. In: Ruiz-García M, Shostell JM, eds. *Molecular population genetics, evolutionary biology and biological conservation of Neotropical carnivores*. New York: Nova Publishers, 187–244

Ruiz-García M, **Pinedo-Castro M**, **Shostell J. 2017.** Small spotted bodies with multiple specific mitochondrial DNAs: existence of diverse and differentiated tigrina lineages or species (*Leopardus* spp: Felidae, Mammalia) throughout Latin America. *Mitochondrial DNA Part A* **29:** 993–1014.

Ruzzante DE, **Walde SJ**, **Gosse JC**, **Cussac VE**, **Habit E**, **Zemlak TS**, **Adams EDM. 2008.** Climate control on ancestral population dynamics: insight from Patagonian fish phylogeography. *Molecular Ecology* **17:** 2234–2244.

Santos A, **Trigo TC**, **Gomes de Oliveira T**, **Silveira L**, **Eizirik E. 2018.** Phylogeographic analyses of the pampas cat (*Leopardus colocola*; Carnivora, Felidae) reveal a complex demographic history. *Genetics and Molecular Biology* **41: 1**(suppl): 273–287.

Sérsic AN, **Cosacov A**, **Cocucci AA**, **Johnson LA**, **Pozner R**, **Avila LJ**, **Sites JR**, **Morando M. 2011.** Emerging phylogeographical patterns of plants and terrestrial vertebrates from Patagonia. *Biological Journal of the Linnean Society* **103:** 475–494.

Swofford DL. 1998. *PAUP*. Phylogenetic analysis using parsimony (*and other methods). Version 4*. Sunderland: Sinauer Associates.

Trigo TC, **Freitas TRO**, **Kunzler G**, **Cardoso L**, **Silva JCR**, **Johnson WE**, **O'Brien SJ**, **Bonatto SL**, **Eizirik E. 2008.** Inter-species hybridization among Neotropical cats of the genus *Leopardus*, and evidence for an introgressive hybrid zone between *L. geoffroyi* and *L. tigrinus* in southern Brazil. *Molecular Ecology* **17:** 4317–4333.

Trigo TC, **Schneider A**, **de Oliveira TG**, **Lehugeur LM**, **Silveira L**, **Freitas TR**, **Eizirik E. 2013.** Molecular data reveal complex hybridization and a cryptic species of neotropical wild cat. *Current Biology* **23:** 2528–2533.

Turchetto-Zolet AC, **Pinheiro F**, **Salgueiro F**, **Palma Silva C. 2013.** Phylogeographical patterns shed light on evolutionary process in South America. *Molecular Ecology* **2:** 1193–1213.

Warren DL, **Glor RE**, **Turelli M. 2010.** ENMTools: a toolbox for comparative studies of environmental niche models. *Ecography* **33:** 607–611.

Warren DL, **Seifert SN. 2011.** Ecological niche modeling in Maxent: the importance of model complexity and the performance of model selection criteria. *Ecological Applications* **21:** 335–342.

Xie W, **Lewis PO**, **Fan Y**, **Kuo L**, **Chen MH. 2011.** Improving marginal likelihood estimation for Bayesian phylogenetic model selection. *Systematic Biology* **60:** 150–160.

Ximenez A. 1973. Notas sobre félidos neotropicales, III. Contribución al conocimiento de *Felis geoffroyi* D'Orbigny & Gervais, 1844 y sus formas geográficas (Mammalia, Felidae). *Papéis Avulsos de Zoologia* **27:** 31–43.

Ximenez A. 1975. *Felis geoffroyi*. *Mammalian Species* **54:** 1–4.

SUPPORTING INFORMATION

Additional Supporting Information may be found in the online version of this article at the publisher's website.

Table S1: Geographical location and haplotype of the samples included in this study.
Table S2: Percentage contribution of climatic variables to the past and current potential distributions in each one of the three models with the highest AUC values.

SHARED DATA

Sequences are available at GenBank (https://www.ncbi.nlm.nih.gov/genbank/), under Accession Numbers MN793073- MN793128 (NADH)and MN849194 - MN849300 (Control Region).